Supplementary Information

Wiring proton gradients for energy conversion

Xinchen Dai[1], Cesare Berton[2,3], Dong Jun Kim[1] and Cristian Pezzato[2,4]*

[1] School of Chemistry, The University of New South Wales, Sydney, New South Wales 2052, Australia;

[2] Institut des Sciences et Ingénierie Chimiques, École Polytechnique Fédérale de Lausanne, Lausanne, Switzerland;

[3] Present address: Department of Chemistry, University of Zurich, Zurich, Switzerland;

[4] Present address: Laboratory for Macromolecular and Organic Chemistry (MOC), Department of Chemical Sciences, University of Padova, via Marzolo 1, 35131 Padova, Italy. E-mail: cristian.pezzato@unipd.it

Table of Contents

1. General information

All reagents and solvents were purchased from commercial suppliers and used without further purification. Compound **1** was synthesized as described previously by our group[S1] (see the characterization data of the new batch in Section 12 below. H_2O used in all preparations was filtered with a MilliQ-Integral5 purification system (mQ H_2O), whereas MeOH was HPLC grade.

UV-Vis spectra and kinetics were acquired on an Agilent Cary 60 spectrometer equipped with an 18-cell holder coupled to a Huber thermostat, using Suprasil quartz cuvettes (114-QS) from Hellma Analytics.

All pH measurements were performed using a Metrohm Titrando 888 coupled with a Biotrode glass electrode; pH data were processed using the software Metrohm Tiamo Light.

Potassium phosphate buffers from pH 3 to 10 were prepared titrating a solution of H_3PO_4 (100 mM, 1L) with KOH 10 M. Diluted stocks of HCl were used below pH 3. All buffer stocks were stored at room temperature.

Samples photoirradiation was carried out using a Prizmatix FC-LED-500Z high-power LED light sources (λ = 500 nm). Unless stated otherwise, the light beam was delivered by polymer optical fibers (core 1500 μM) i) positioned orthogonally to and just below the liquid/air interface of sample solutions (UV-Vis) or ii) connected to an FCM1-06 collimator coupled with 45° mirror cage, resulting in a light beam tilted by 90° (pH jumps). Power measurements of the fiber-coupled LED output were made with Thorlabs S142C integrating sphere photodiode power sensor; the uncertainty is within ±5%.

Cylindrical cells for photoenergy harvesting experiments were constructed as follow: NMR tubes (Wilmad® 5-mm diam., economy, 0.5 mm wall thickness) were cut into 5-cm long pieces with a diamond glass cutter, and capped with two silicone rubber caps (Uxcell, product number: a23080300ux0073) bearing a coaxially-inserted Pt wire (Goodfellow 99.99%, d = 0.3 mm, annealed); in order for the cells to be filled with photoacid solutions in a controlled manner, a 1-mm hole was drilled with a diamond microdrill on one side of the cells, while a headless NMR tube cap act as movable sealing cover for this hole (see Section 11 for more details).

Electrochemical tests were performed using either a Metrohm Vionic potentiostat or a Keithley 2450 source meter.

2. Data elaboration

UV-Vis analyses and pH measurements were carried out as described previously.[S2] Curve fittings were performed in Excel, using the Solver add-in for minimizing the sum of the square deviations from the corresponding model equation. The equations used are the following:

Apparent acidity constant (Ref. S2)

Eqn. S1:
$$A_{eq} = A_{OH} + \frac{A_H - A_{OH}}{1 + exp\left(\frac{pH - pK_a^{GS/MS}}{P}\right)}$$

First-order equilibration/relaxation kinetics (Ref. S2)

Eqn. S2:
$$A_t = A_{eq} + (A_0 - A_{eq})e^{-k_{obs}t}$$

Observed rate constant of relaxation after light irradiation (Ref. S2)

Eqn. S3:
$$k_{obs,relax} = k_{-2}\left(\frac{K_a^{MS}}{[H^+] + K_a^{MS}}\right)\left(\frac{K_a(1 + K_c) + [H^+]}{[H^+] + K_a}\right)$$

Quantum yield of isomerization (Ref. S3)

Eqn. S4:
$$\Phi = -\frac{dA_{MCH}}{dt}\frac{V\,N_a\,h\,c}{\varepsilon_{MCH}\,d\,\lambda_{ex}\,P_0\,(1 - 10^{-A_{ex}})}$$

Observed rate constant of hydrolysis (Ref. S2)

Eqn. S5:
$$k_{obs,hydr} = \frac{k_w[H^+] + k_{OH}K_w}{([H^+] + K_a^{GS})\left(\frac{k_{-w}}{k_h}[H^+] + 1\right)}$$

2. pK_a^{GS} *vs.* % MeOH v/v

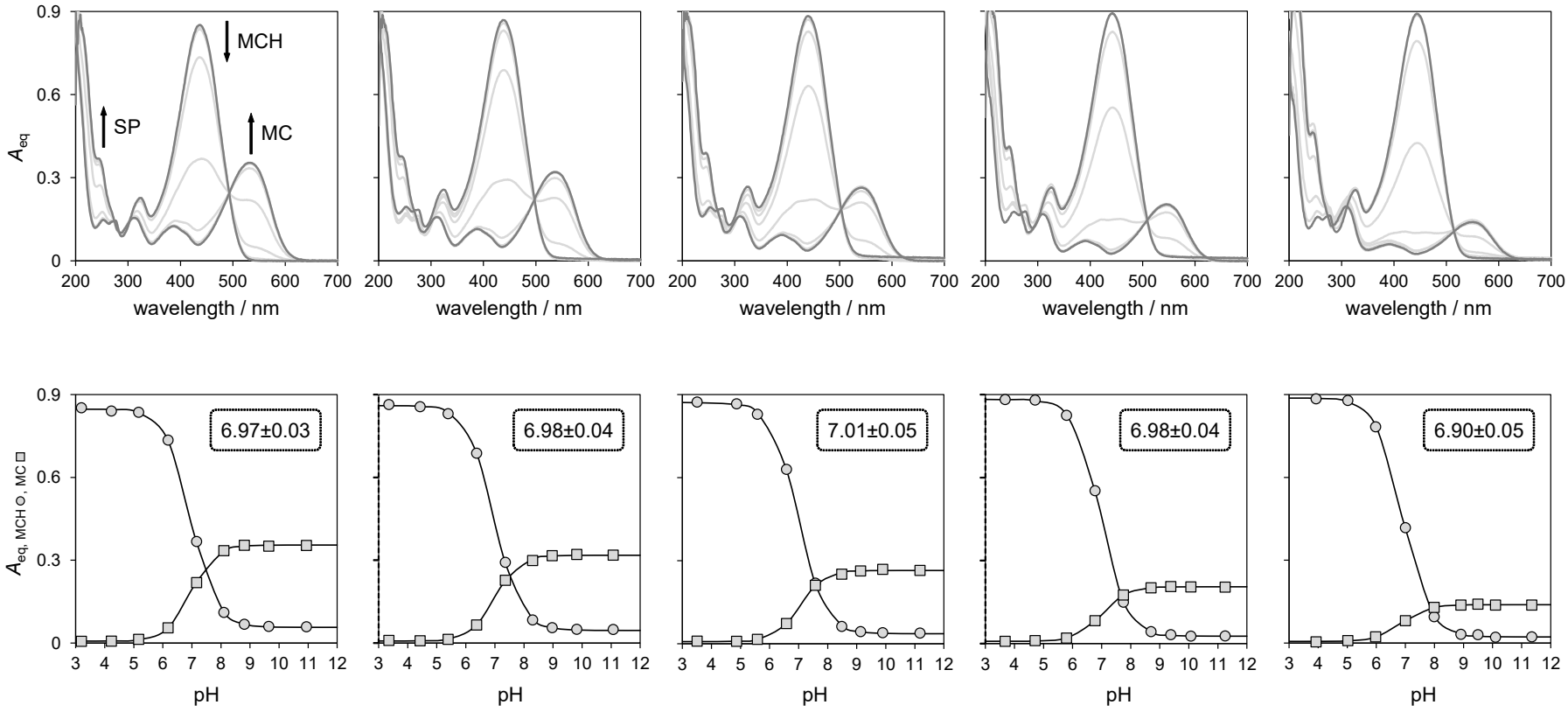

Figure S1. UV-Vis pH titrations as a function of the pH (top) and corresponding pH-dependent profiles of $A_{eq, MCH}$ and of $A_{eq, MC}$ (bottom); solid black lines represent the best fit to eqn. S1. Experimental conditions: [**1**] = 29 ± 1 μM, [phosphate buffer] = 20 mM, T = 25 °C, solvent composition (from left to right): 0, 10, 20, 30, and 40% MeOH v/v.

3. λ_{max} of MCH and MC *vs.* % MeOH v/v

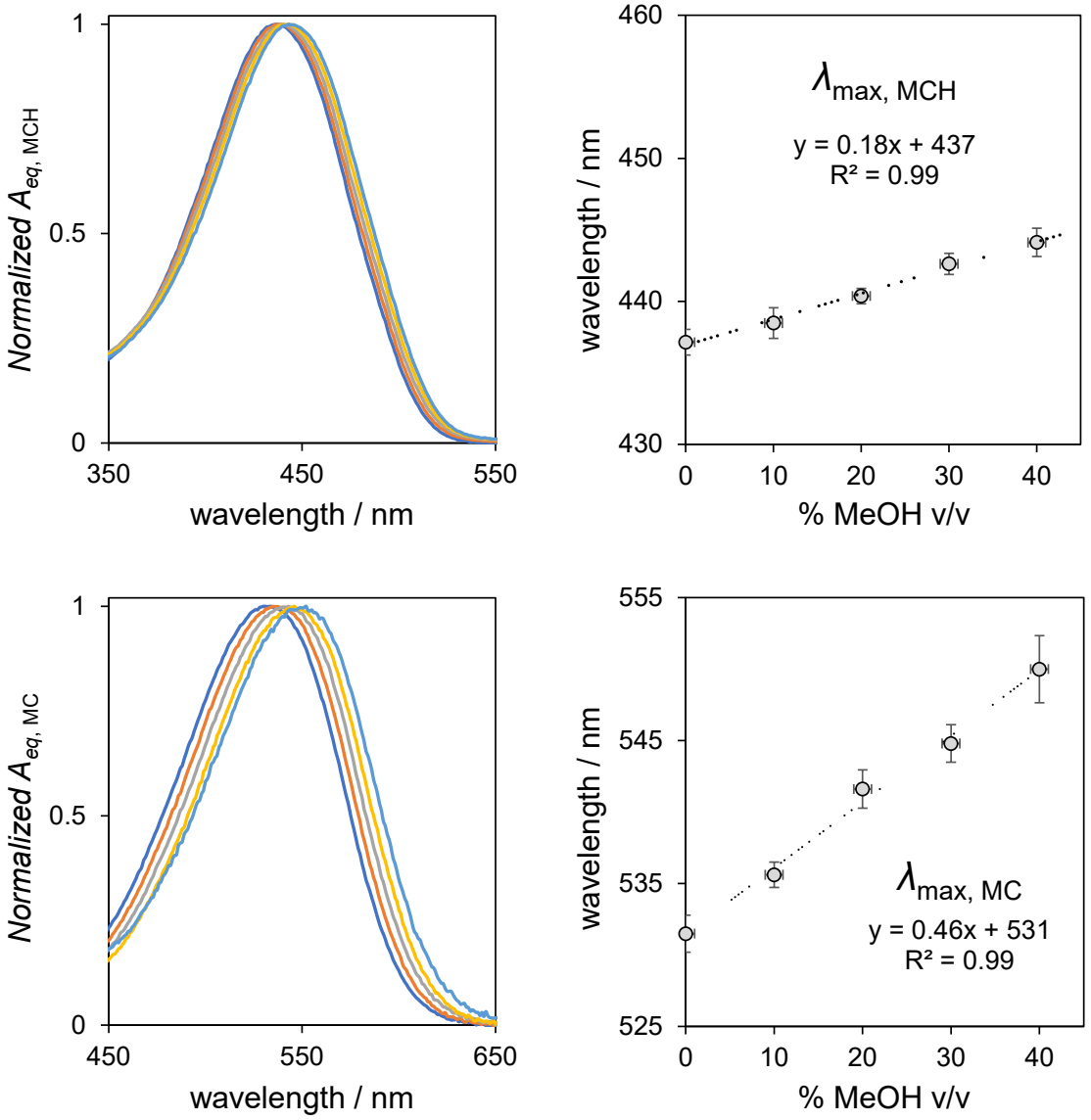

Figure S2. Normalized absorption of MCH (top) and MC (bottom) at equilibrium and corresponding bathochromic shift as a function of % MeOH v/v. These data were processed considering the absorption spectra at low and high pH obtained in the UV-Vis pH titrations above (Figure S1).

4. Equilibration kinetics of MC *vs.* % MeOH v/v

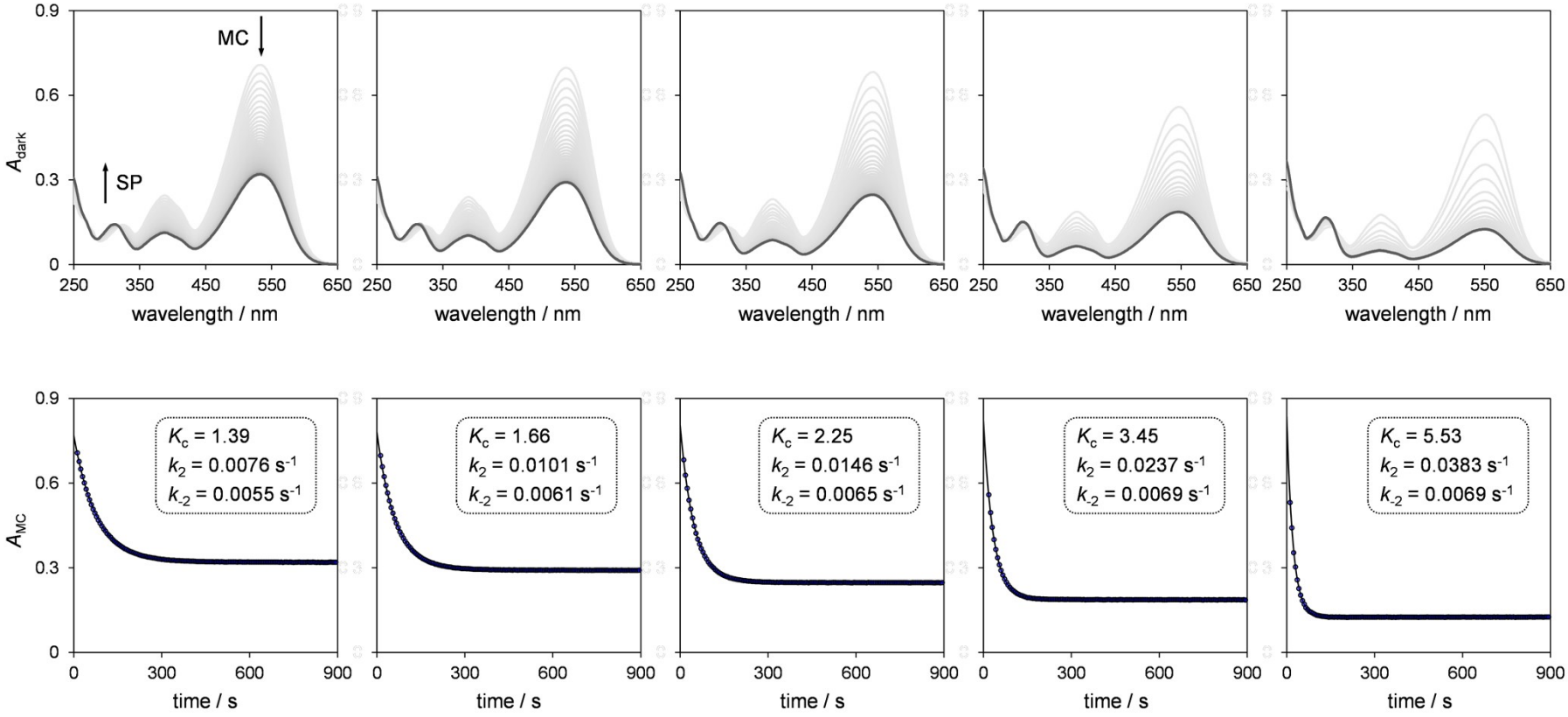

Figure S3. Absorption profiles as a function of time (top) and equilibration kinetics of the MC band (bottom) after on-site addition and rapid mixing of an aliquot (50 µL) of a solution (0.5 mM in mQ water) of compound **1** into a cuvette containing the buffer solution (950 µL) at the desired solvent composition; solid black lines represent the best fit to eqn. S2. Experimental conditions: [**1**] = 29 ± 1 µM, [phosphate buffer] = 20 mM, pH 10, T = 25 °C, solvent composition (from left to right): 0, 10, 20, 30, and 40% MeOH v/v.

5. pK_a *vs.* % MeOH v/v

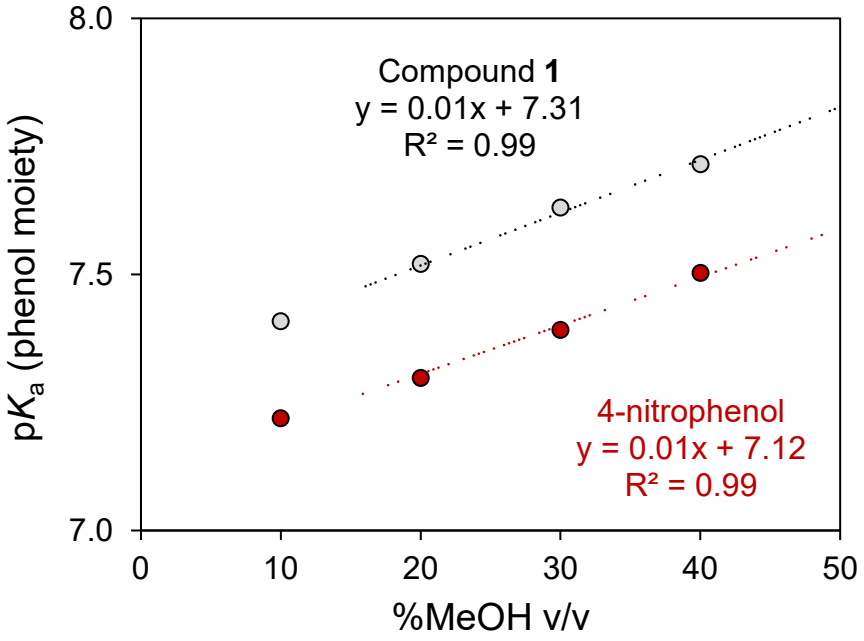

Figure S4. Extrapolated pK_a of compound **1** as a function of solvent composition reported together with that of 4-nitrophenol (values taken form Ref. 47 of the main text).

6. pK_a^{MS} *vs.* % MeOH v/v

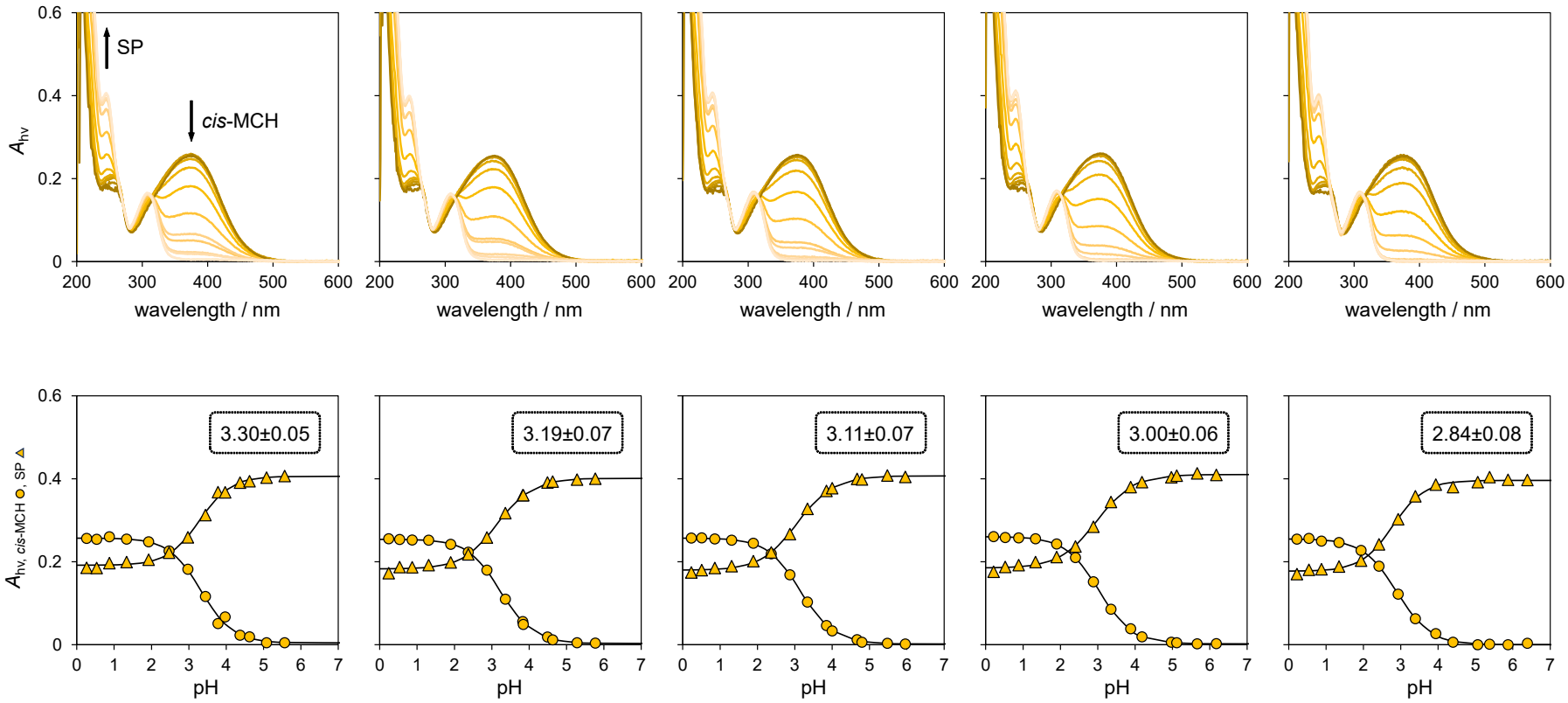

Figure S5. UV-Vis pH titrations as a function of the pH (top) and corresponding pH-dependent profiles of $A_{hv,\ cis\text{-}MCH}$ and $A_{hv,\ SP}$ (bottom); solid black lines represent the best fit to eqn. S1. Experimental conditions: [**1**] = 29 ± 1 μM, [phosphate buffer] = 20 mM (4 < pH < 7), HCl solutions (pH < 4), T = 25 °C, 500 nm LED-light (90 mW), solvent composition (from left to right): 0, 10, 20, 30, and 40% MeOH v/v.

7. Relaxation and isomerization kinetics *vs.* % MeOH v/v

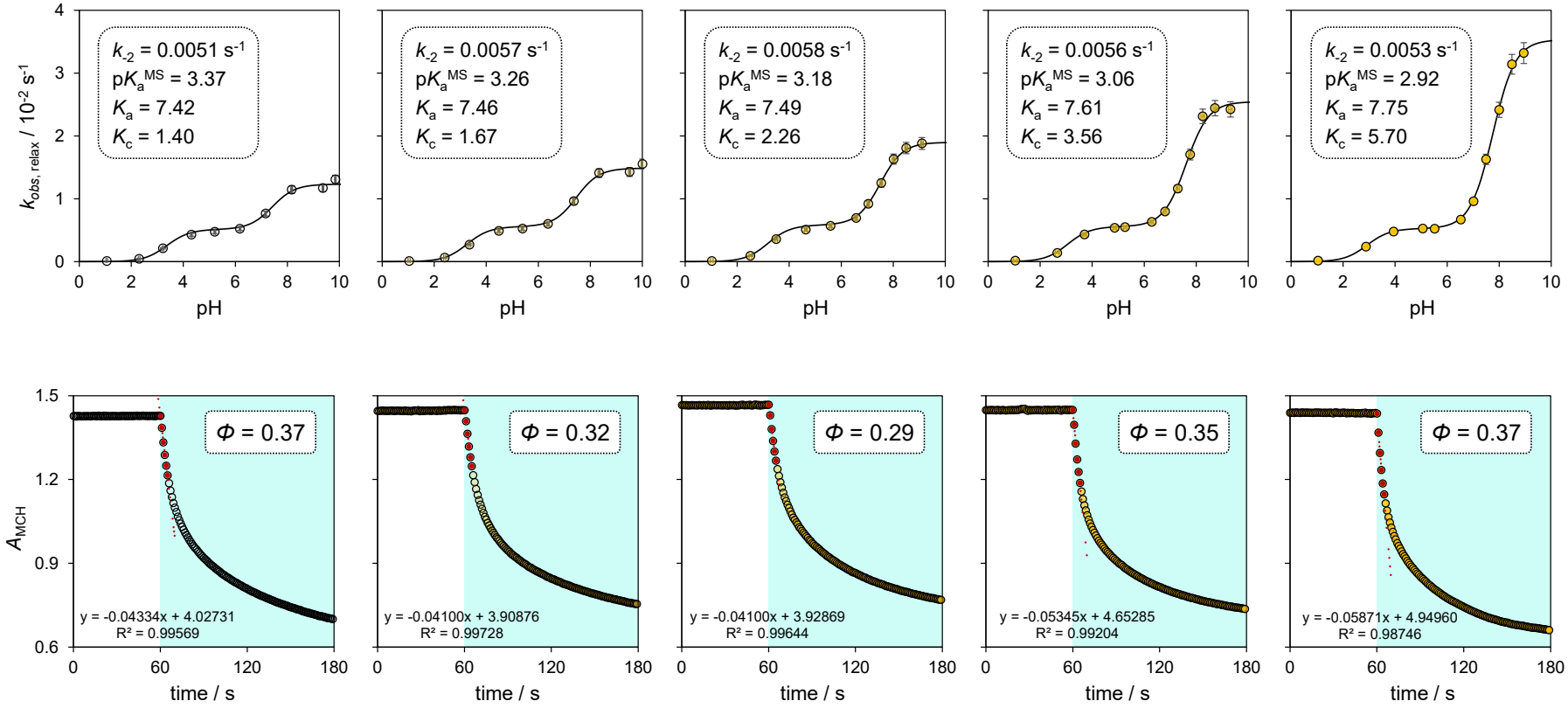

Figure S6. Relaxation kinetics irradiation in situ as a function of the pH (top) and isomerization kinetics at pH 4.5 during 500 nm light irradiation (bottom); solid black lines represent the best fit to eqn. S3; the initial rate (dA_{MCH}/dt) of MCH-to-SP isomerization is calculated by a linear fitting of the first points up to $R^2 \geq 0.99$; Φ values are then determined considering eqn. S4, with V = 0.001 L, ε_{MCH} = 30350 L mol^{-1} cm^{-1}, d = 1 cm, λ_{ex} = 500 nm, and P_0 = 2 mW; all kinetics were acquired at λ = 437 nm, so the absorbance of the system at λ_{ex} ($A_{ex} = A_{500}$) was determined considering the ratio A_{500} / A_{437} in the corresponding spectrum of MCH at low pH (see Figure S1). Experimental conditions: [**1**] = 29 ± 1 μM (relaxation) or 50 ± 2 μM, [phosphate buffer] = 20 mM (4 < pH < 7), HCl solutions (pH < 4), T = from 25 °C, 500 nm LED-light (90 mW or P_0 = 1 mW, respectively), solvent composition (from left to right): 0, 10, 20, 30, and 40% MeOH v/v.

8. Hydrolysis *vs.* % MeOH v/v

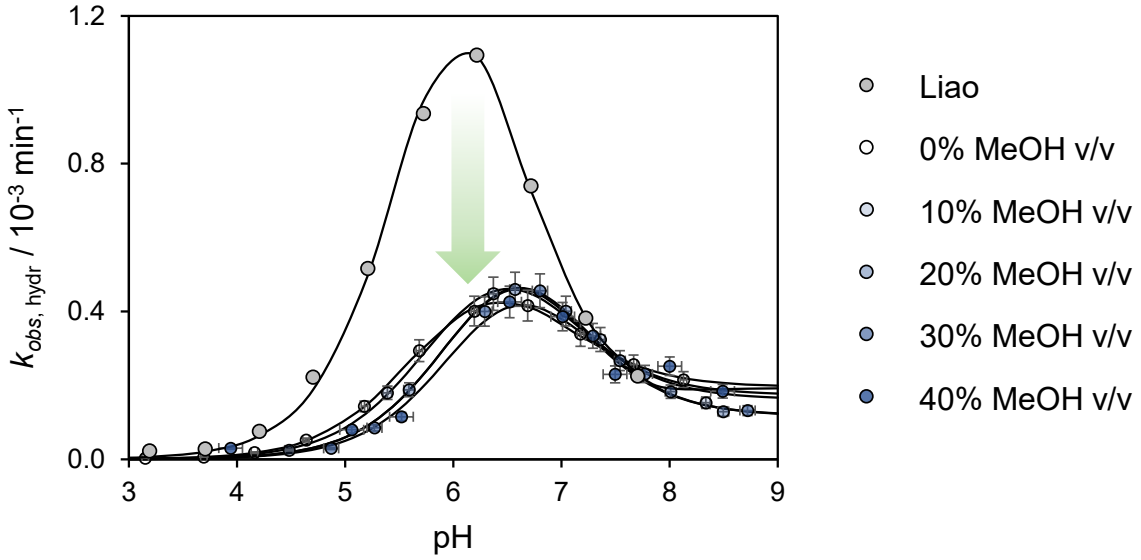

Figure S7. Hydrolysis profiles as a function of the pH and the MeOH content plotted together with that of Liao's photoacid (i.e., the parent compound lacking the -OMe group in *para*-position of the indolenine side; solid black lines represent the best fit to eqn. S5; Experimental conditions: [**1**] = 29 ± 1 μM [phosphate buffer] = 20 mM, *T* = from 25 °C.

9. Photochemical apparatus

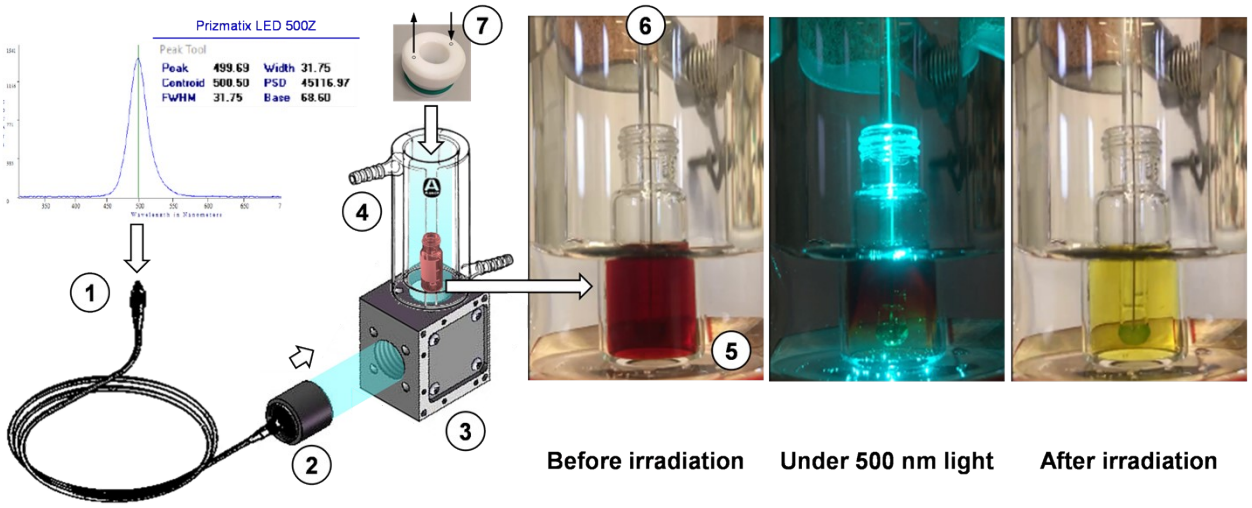

Figure S8. The photochemical apparatus designed for performing pH jump studies.[S2]

Our apparatus is composed as follows: fiber-coupled 500 LED-light source (1) ending with a 2.5 cm collimator (2) mounted on a 45° mirror cage (3), which drives the light beam parallel to 50-mL jacketed beaker (4) connected to a thermostat. MS vials containing 1 mL of buffer solution are placed coaxially (in the beaker containing 8 mL of water as bath, 5) before a Metrohm Biotrode glass electrode (6) is inserted from the top through a custom-made Teflon cap equipped with inlet/outlet for inert gas (7). On the right: representative pictures of a light-switchable buffer under operative conditions.

10. Preparation of light-switchable buffers

Saturated solution of compound **1** were prepared by stirring (cross-shaped stir bar, 300 rpm) an excess amount of crystals into 10-mL 40% aqueous MeOH mixtures containing HCl (C_{HCl} = 1 mM → S_{MCH}) or increasing amount of NaOH ($C_{NaOH} = \alpha \cdot S_{MCH}$, $0 < \alpha < 2$). We employed the jacketed beaker in the photochemical apparatus above for maintaining the temperature constant during the experiment (T = 25 °C) and monitoring the pH of the solution upon dissolution of **1** in the dark. The obtained suspensions are then microfiltered (0.22 μm) and analyzed by UV-Vis to calculate the saturation concentration (S_{TOT}, Fig 5b in the main text) prior to pH jump analyses. To convert absorbances into concentrations we used molar extinction coefficient (ε_{MCH}, pH 3) reported previously (see Ref. S1). The resulting pH profiles upon solubilization and pH jumps under 500 nm light irradiation are reported below.

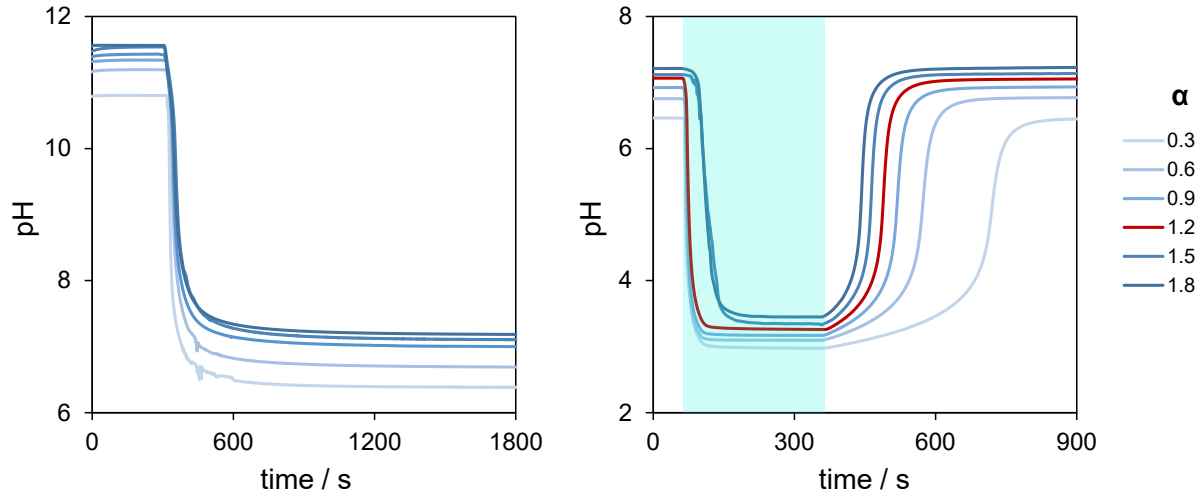

Figure S9. pH stabilization upon dissolution of **1** in 40% MeOH v/v containing sub-stoichiometric amount of NaOH (left) and corresponding pH jumps upon 500 nm light irradiation (0.93 W cm^{-2}). The red line indicates the best-performing light-switchable buffer in terms (α = 1.2, ΔpH = 3.8).

11. Electrochemical studies

11.1 General remarks

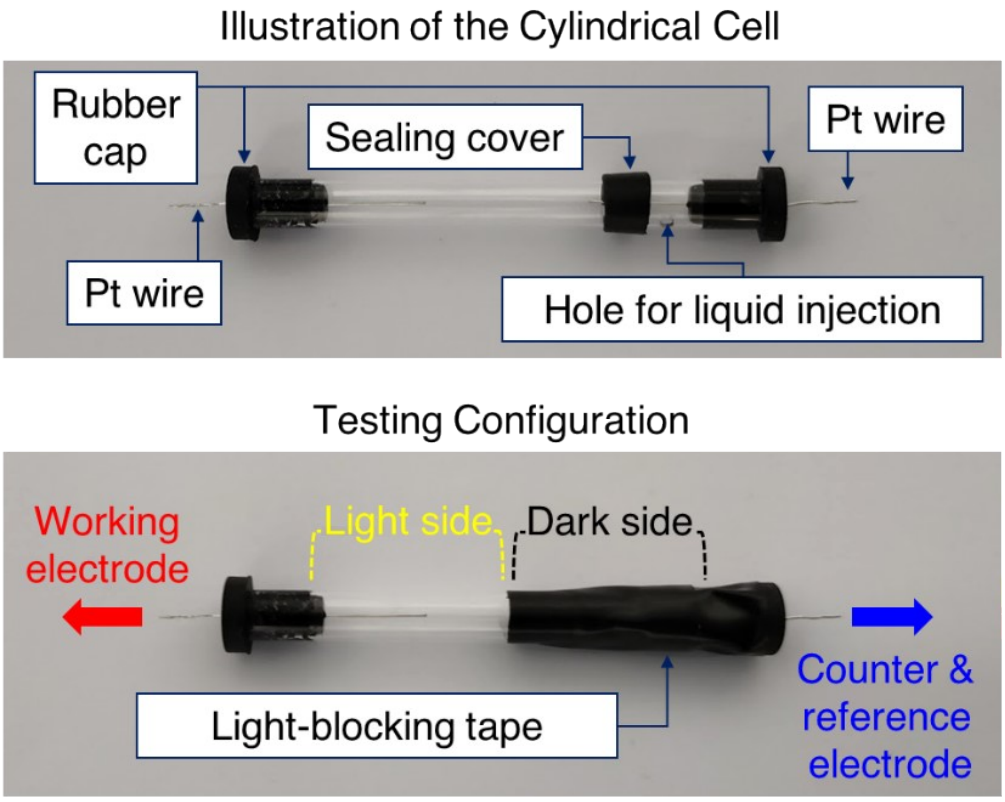

Figure S10. Illustration of the cylindrical cell (top) and the testing configuration (bottom) for electrochemical studies. Deep color photoacid solution was not installed in the lower illustration to display a better contrast.

Cleaning procedures for cylindrical cell. Acetone was injected into the cell followed by ultrasonication for 10 minutes to remove the impurity inside. Afterward, the cell was rinsed by acetone three times. Use a heat blower to dry the cell until all the acetone evaporates. Blow Argon gas to replace the residual gaseous acetone inside of the cell. 0.1 M H_2SO_4 solution was injected into the cell for electrochemical cleaning and activation of Pt electrodes. The cleaning was performed by cyclic voltammetry scanning from 1 to –1 V for 40 cycles in a two-electrode setup. The redox current become stable after 40 cycles, which indicates the Pt was cleaned and activated.[S4] Remove H_2SO_4 solution and rinse cell with acetone three times. Dry the cell using heat blower

until all the acetone evaporates. Blow Argon to replace the residual gaseous acetone inside of the cell. The cell is ready for electrochemical tests.

Making a photoacid cell (PAC). The photoacid solution for electrochemical studies was prepared as described in Section 10. We used the solution at α = 1.2 (S_{TOT} = 7.6 ± 0.4 mM), which led to the optimum ΔpH of 3.8 upon irradiation. The solution was degassed for 5 min in an ultrasonication bath and then injected into the cylindrical cell. The movable sealing cover was moved to cover the injection hole, followed by masking half of the cylindrical cell with a light-blocking tape.

Electrochemical measurement protocol. Before any electrochemical test, the cell was short-circuited to remove any static charge on the electrodes. The testing configuration and electrode connection of the photoacid cell is shown in Figure S10. Open-circuit voltage and short-circuit current were recorded separately by a Metrohm Vionic potentiostat. All measurements were performed at an ambient temperature of 22 °C.

Irradiation conditions for electrochemical studies. For the tests under dark condition, the cylindrical cell was covered by aluminum to avoid absorption of room light. For the tests under light, same light source as the pervious photochemistry studies was used, i.e., Prizmatix FC-LED-500Z high-power LED light sources (λ = 500 nm). The light beam was delivered by polymer optical fibers (core 1500 μM) connected to an FCM1-06 collimator and put above the cylindrical cell. Various irradiance were achieved by adjusting the power of the light beam and the distance between the collimator and the cell.

11.2 Validation of the PAC mechanism

This light-induced voltage of PAC is attributed to the establishment of an electrochemical potential difference between two Pt wires surrounded by photoacid solution at different acidity. The relation could be expressed by the Nernst equation[S5]:

Eqn. S6:
$$\Delta E = \frac{RT}{zF} ln\left(\frac{[H^+]^{hv}}{[H^+]^{dark}}\right) = \frac{2.303RT}{F}\left(pH^{dark} - pH^{hv}\right) \approx 0.0002 \cdot T \cdot \Delta pH\ (Volts)$$

where ΔE, R, T, z, and F represent the cell potential, the gas constant, the temperature, the number of electrons transferred, and the Faraday constant, respectively. The time derivative of ΔE is

derived as follows, assuming that the proton concentration in the dark side does not change over time:

Eqn. S7: $$\frac{\partial \Delta E}{\partial t} = \frac{\partial}{\partial t}\left[\frac{RT}{zF}\left(ln[H^+]^{h\nu} - ln[H^+]^{dark}\right)\right] = \frac{RT}{zF}\frac{\partial ln[H^+]^{h\nu}}{\partial t} \approx \frac{RT}{F}k_H$$

The assumption above ($[H^+]^{dark} \approx$ const.) is valid when taking initial rates as case study – i.e., the theoretical mean square displacement of protons through the cell is well below the distance between the two electrode ($x = \sqrt{2Dt} < 16$ mm).

In the case of the pH jump studies, k_H is calculated considering the time derivative of ΔpH as follows:

Eqn. S8: $$\frac{\partial \Delta pH}{\partial t} = -2.303\frac{\partial}{\partial t}\left(ln[H^+]^{dark} - ln[H^+]^{h\nu}\right) = 2.303\frac{\partial ln[H^+]^{h\nu}}{\partial t} \approx 2.303k_H$$

using the pH jump profiles reported above (Fig. S8, right). The k_H values obtained with Eqn S7 and S8 are reported below on the left and on the right, respectively, as function of N_λ/N.

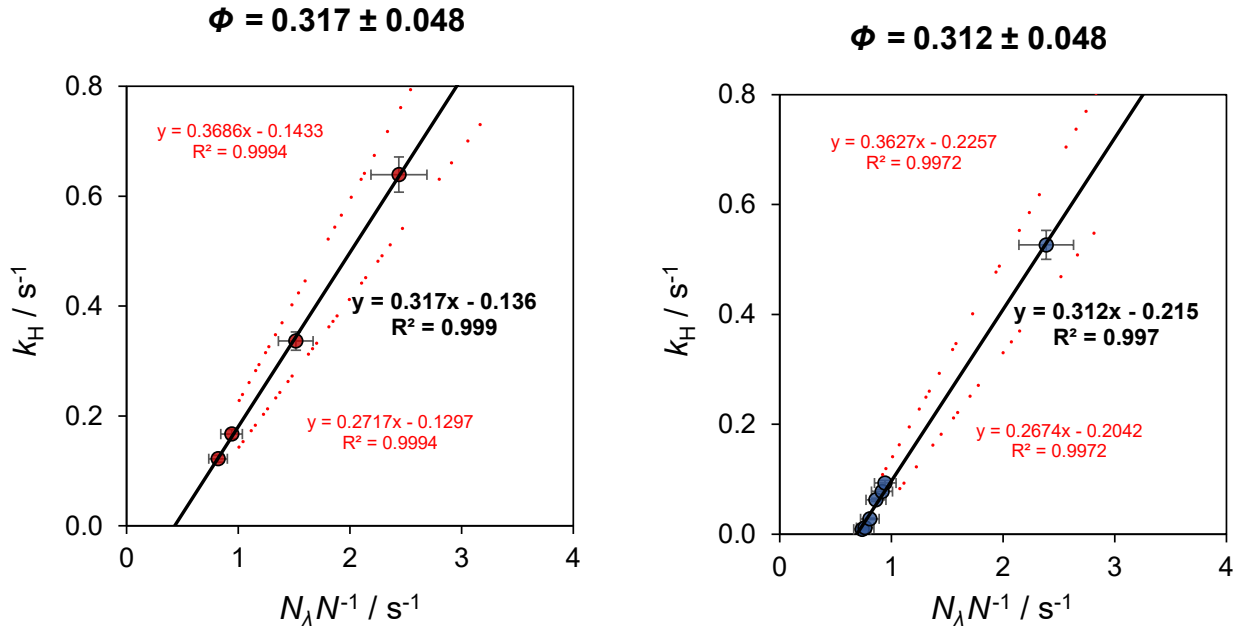

Figure S11. Observed rate constant of proton release in variable-irradiance V_{OC} (left) and pH-jumps (right) experiments as a function of the photon flux (N_λ = Irradiance·A·λ_{ex} / hc) normalized for the total number of molecules in solution ($N = S_{TOT}\cdot V\cdot N_a$). Dotted red lines represent the upper/lower boundaries based on the error on the x- and y-axis.

11.3 Calculation of the A/V ratio

In the photochemical reactor for studying the pH jumps, we have a 2 mL clear glass vial filled with 1 mL of photoacid solution. Light arrives from the bottom hitting an area of $\pi * (10\ mm / 2)^2 = 78.5\ mm^2$. Thus, the A/V for pH jump measurements is $78.5\ mm^2 / 1000\ mm^3 = 0.079\ mm^{-1}$.

In the case of the photoacid cell, the detailed parameters were described previously. We have half of the cell (ID = 4 mm) that is irradiated, so in total $\pi * (4\ mm / 2)^2 * (50\ mm / 2 - 7\ mm) = 226\ mm^3$ solution is considered undergoing light reaction. The area perpendicular to the light beam is $(50\ mm / 2 - 7\ mm) * 4\ mm = 72\ mm^2$. The A/V ratio is $72\ mm^2 / 226\ mm^3 = 0.318\ mm^{-1}$.

A/V (photoacid cell) / A/V (photochemical reactor) = $0.318\ mm^{-1} / 0.079\ mm^{-1} = 4.0$.

11.4 Short-circuit current studies

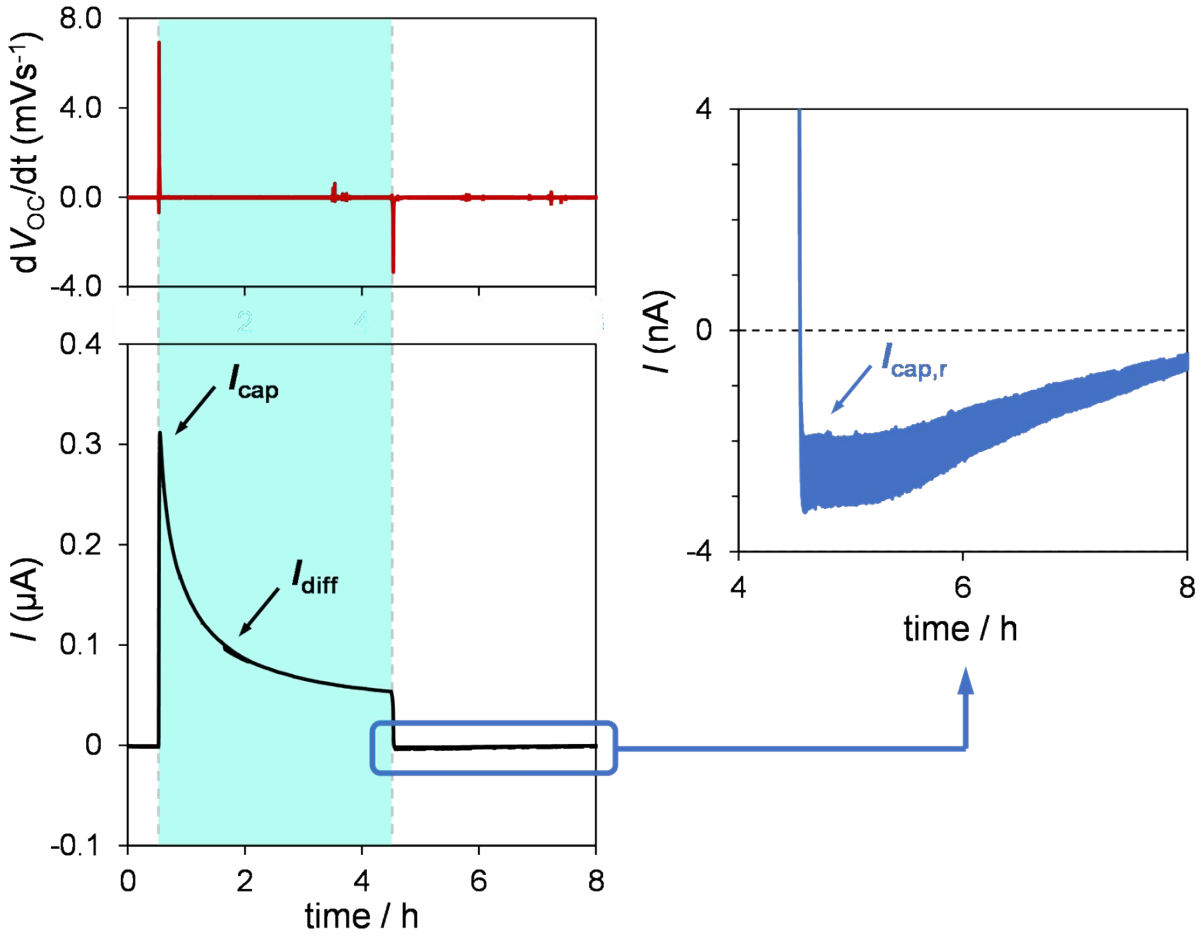

Figure S12. Current profile against the corresponding dV_{OC} /dt plot under light irradiation (left) and current recovery under dark conditions (right) obtained for the optimized light-switchable buffer solution. Experimental conditions: [**1**] = 7.6 ± 4 mM, α = 1.2, T = 22 °C, 500 nm LED-light: 6 mW cm^{-2}.

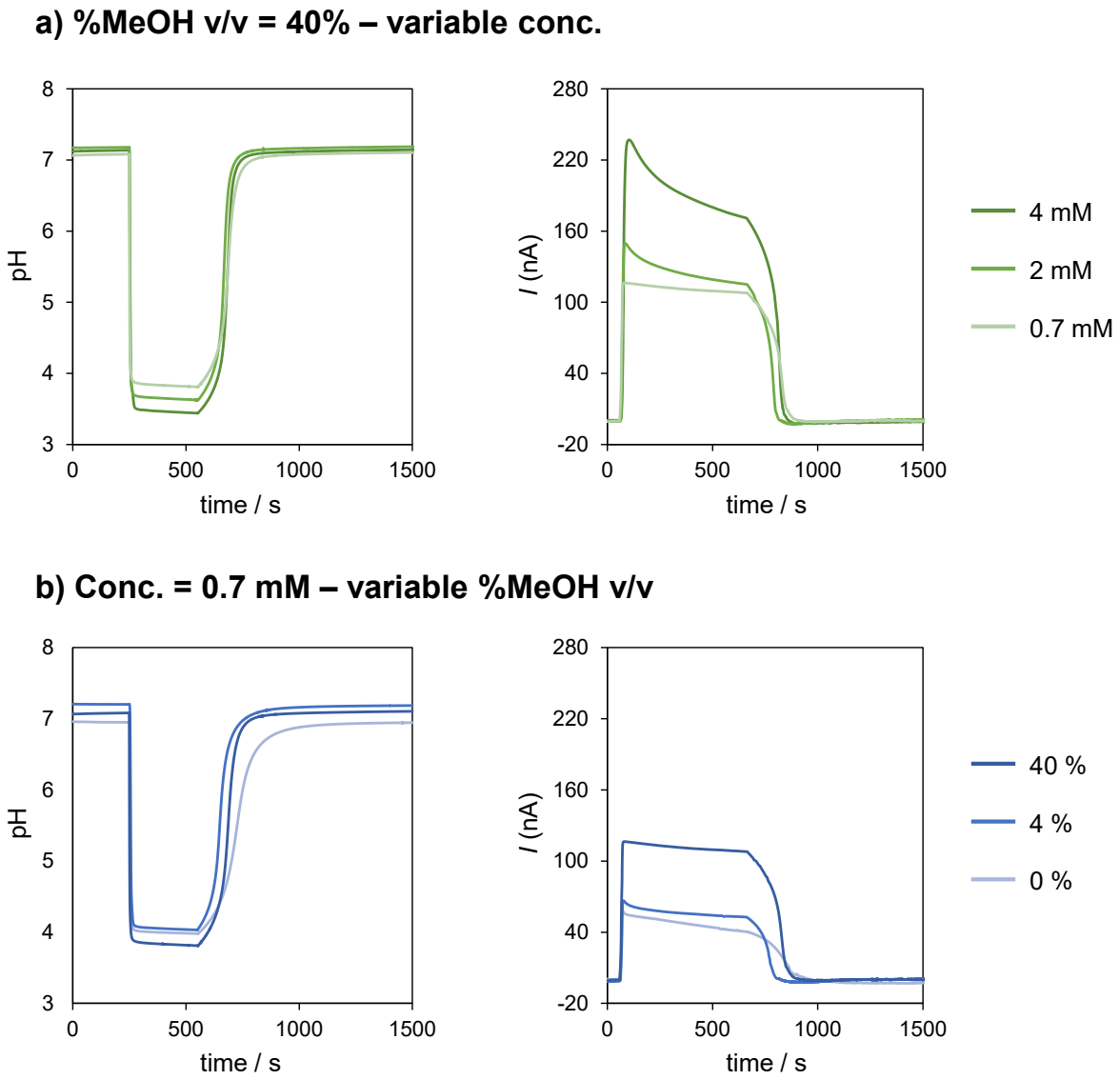

Figure S13. pH jumps tests and corresponding current profiles as a function of (a) the concentration of the buffer, and (b) the % MeOH v/v. The concentation of **1** was regulated by diluting the optimized light-switchable buffer solution (7.6 ± 4 mM, α = 1.2) using: (a) H_2O/MeOH 6:4 or (b) H_2O/MeOH 6:4 and water. Experimental conditions: T = 22 °C, 500 nm LED-light: 6 mW cm^{-2}.

12. Characterization of compound 1

^{1}H NMR (400 MHz, DMSO-d_6) δ (ppm): 10.92 (s, 1H), 8.50 (d, $^{3}J_{trans}$ = 16.4 Hz, 1H), 8.24 (d, ^{3}J = 8.0 Hz, 1H), 7.95 (d, ^{3}J = 8.8 Hz, 1H), 7.81 (d, $^{3}J_{trans}$ = 16.4 Hz, 1H), 7.51 (d, ^{4}J = 2.4 Hz, 1H), 7.44 (t, ^{3}J = 7.8 1H), 7.17 (dd, ^{3}J = 8.8, ^{4}J = 2.4 Hz, 1H), 7.02 (d, ^{3}J = 8.0 Hz, 1H), 6.97 (t, ^{3}J = 7.6 Hz, 1H), 4.77 (t, ^{3}J = 6.8 Hz, 2H), 3.89 (s, 3H), 2.63 (t, ^{3}J = 6.8 Hz, 2H), 2.16 (p, ^{3}J = 6.8 Hz, 2H), 1.76 (s, 6H).

^{13}C NMR (101 MHz, DMSO-d_6) δ (ppm): 179.48, 160.72, 158.62, 146.73, 145.70, 135.17, 134.18, 129.53, 121.41, 119.99, 116.54, 116.23, 114.86, 111.56, 108.84, 56.13, 51.82, 47.31, 45.58, 26.43, 24.71.

HRMS (ESI+) m/z: $[M + H]^+$ Calcd for $C_{22}H_{26}NO_5S^+$ 416.153; Found 416.154.

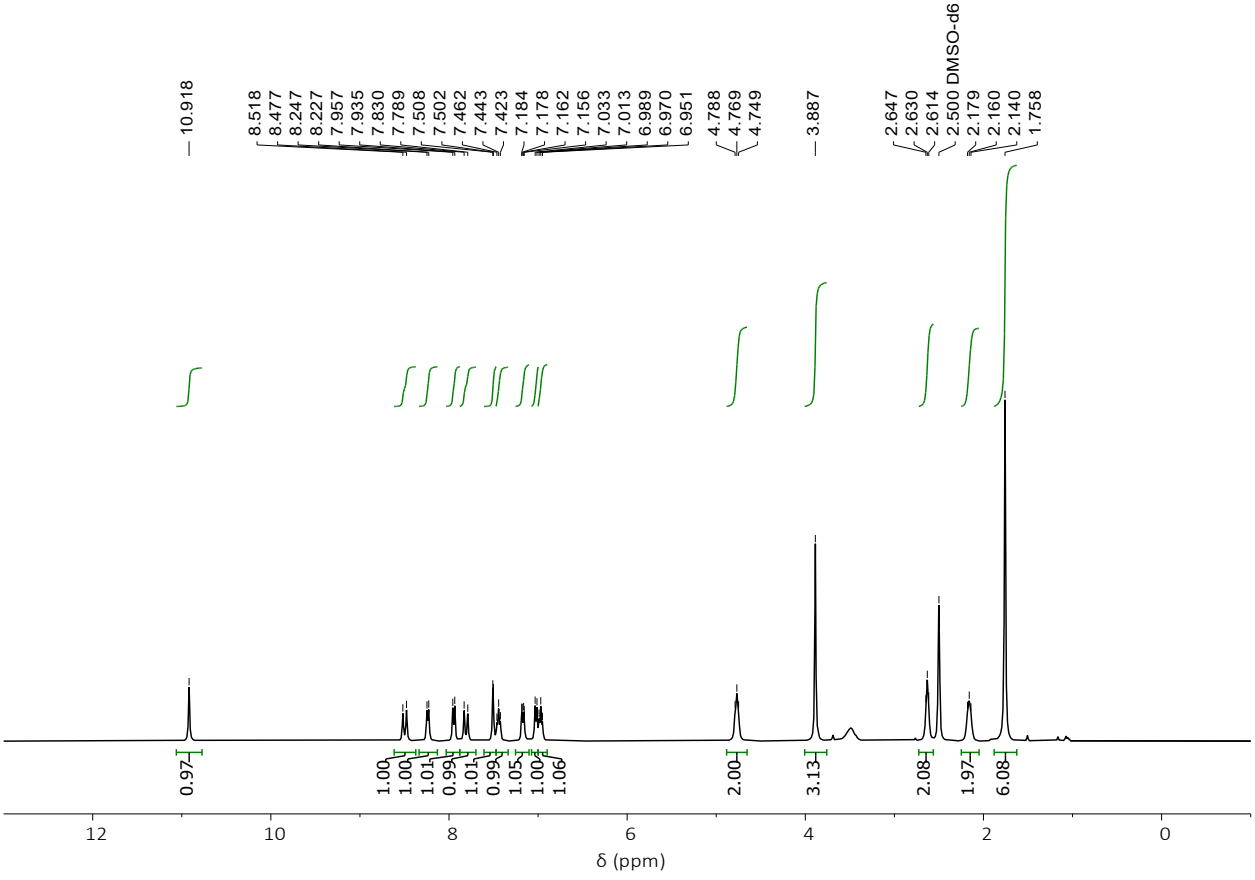

Figure S14. ^{1}H NMR (400 MHz, DMSO-d_6) of compound **1**.

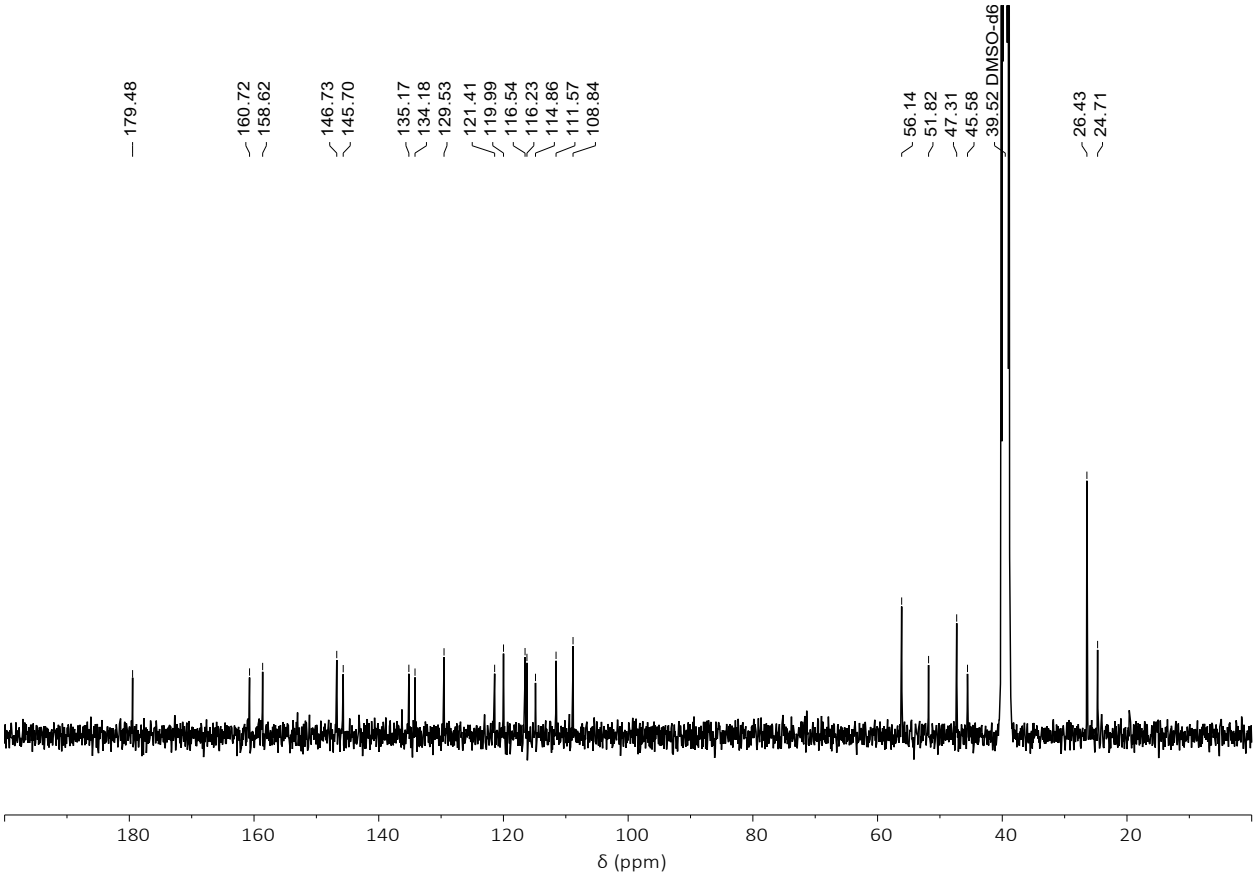

Figure S15. ^{13}C NMR (101 MHz, DMSO-d_6) of compound **1**.

13. References

1. Berton, C.; Busiello, D. M.; Zamuner, S.; Scopelliti, R.; Fadaei-Tirani, F.; Severin, K.; Pezzato, C., Light-switchable buffers. *Angew. Chem. Int. Ed.* **2021**, *60*, 21737-21740.
2. Berton, C.; Busiello, D. M.; Zamuner, S.; E. Solari, Scopelliti, R.; Fadaei-Tirani, F.; Severin, K.; Pezzato, C., Thermodynamics and kinetics of protonated merocyanine photoacids in water. *Chem. Sci.* **2020**, *11*, 8457-8468.
3. Halbritter, T.; Kaiser, C.; Wachtveitl, J.; Heckel, A., Pyridine-spiropyrans derivative as a persistent, reversible photoacid in water. *J. Org. Chem.* **2017**, *82*, 8040-8047.
4. James, S.D., The electrochemical activation of platinum electrodes. *J. Electrochem. Soc*. **1967**, *114*, 1113.
5. Bard, A. J.; Faulkner, L. R., Electrochemical Methods : Fundamentals and Applications., 2nd ed.; John Wiley & Sons, Incorporated: Hoboken, NJ, **2000**.